8602 *J. Am. Chem. Soc.* **1991**, *113*, 8602-8611

A Comparative Theoretical Analysis of the Physicochemically Dissimilar Tetrathiolate- and Oxalate-Bridged Dititanium Series, $[(Cp_2Ti)_2(\mu\text{-}C_2X_4)]^n$ (Where X = S, n = 0, 1−, 2−; X = O, n = 0, 2+): An Explanation of Electron Delocalization from the Metal Centers Upon Replacement of the Oxalate Ligand with the Tetrathiooxalate Ligand

Holly Ann Harris,[1a] **David R. Kanis,**[1b] **and Lawrence F. Dahl***

Contribution from the Department of Chemistry, University of Wisconsin—Madison, Madison, Wisconsin 53706. *Received August 25, 1989*

Abstract: Although electronically equivalent with the oxalate-bridge $(Cp_2Ti)_2(\mu\text{-}C_2O_4)$ (**2**) and the corresponding nitrogen-containing $(Cp_2Ti)_2(\mu\text{-}C_2(NR)_4)$ (**3**), the tetrathiolate-bridged $(Cp_2Ti)_2(\mu\text{-}C_2S_4)$ (**1**) (where Cp denotes $\eta^5\text{-}C_5H_5$) exhibits sharply contrasting magnetic and electrochemical behavior at room temperature. **1** is diamagnetic and displays two quasi-reversible one-electron reductions, whereas **2** and **3** are paramagnetic (with two unpaired electrons) and only undergo single two-electron oxidations. The geometry of the $TiX_2C_2X_2Ti$ core in **1** (X = S) also differs markedly from those in **2** (X = O) and **3** (X = NR) in that its C_2X_4 bridging ligand possesses a significantly shorter C–C bond (viz., 1.41 Å in **1** vs 1.523 (11) Å in **2** and 1.504 (6) Å in **3**) and the folding angles (α) of the two TiX_2 planes out of the $X_2C_2X_2$ plane are much larger (viz., 46.5° (trans) in **1** vs 11.4° (cis) in **2** and 11.1° (trans) in **3**). Molecular orbital calculations were carried out with the parameter-free Fenske-Hall model on the tetrathiolate-bridged **1**, the oxalate-bridged **2**, and their hypothetical ions. In order to assess the effects of change of geometry upon electronic structure, calculations were also performed on several alternative configurations of **1** and **2** (viz., C_{2v} cis and C_{2h} trans isomers of **2** with α = 11.4°; C_{2h} trans isomers of **1** and **2** with α = 0.0°, 11.4°, and 46.5°). These calculations provide a quantitative electronic basis for the stereophysical differences arising from the formal replacement of the first-row oxygen atoms in the bridging C_2X_4 ligand in **2** with less electronegative sulfur atoms in **1**. A low-energy π-acceptor C_2S_4 orbital (corresponding to the b_{3u} LUMO for "free" $C_2S_4^{2-}$ under D_{2h} symmetry) is the main contributor (60%) to the filled HOMO and is therefore responsible for the extensive electron delocalization from the metal centers in **1**. The strong bonding interactions of this π-acceptor C_2S_4 orbital with the antisymmetrical dititanium symmetry combination of the valence $d_{x^2-y^2}/d_{z^2}$ Ti AOs produces a nondegenerate HOMO that accounts for the spin pairing of the unpaired electron on each Ti in **1**. In contrast, the corresponding higher energy π-acceptor $C_2O_4^{2-}$ orbital in **2** is energetically inaccessible such that the symmetrical and antisymmetrical dititanium combinations of the $3d_{x^2-y^2}/3d_{z^2}$ Ti AOs form an accidentally degenerate set of half-occupied HOMOs. This MO representation is completely consistent with the valence-bond description in which **2** possesses an electron-localized configuration involving the interaction of a $C_2O_4^{2-}$ dianion with two d^1 Ti(III) Cp_2Ti^+ fragments. Atomic charge calculations obtained by the natural bond orbital method gave a significantly greater total negative charge for the C_2S_4 ligand in **1** than for the C_2O_4 ligand in **2**. This negative charge difference is compatible with the C_2S_4 ligand formally possessing a nonintegral oxidation state between a dianion (2−) and a tetraanion (4−); this result is also in agreement with the determined C–C distance (1.41 Å) in **1**, which is intermediate between single-bond and double-bond distances. The geometry of the $TiS_2C_2S_2Ti$ core in **1** is strongly dependent on metal orbital overlap with the C_2S_4 π orbitals (especially the HOMO); the large folding angles (α = 46.5°) represent an optimized balance of angular-dependent Ti–S σ- and π-type interactions. The near-planar geometry of the $TiO_2C_2O_2Ti$ core in **2** is due to the Ti–O interactions being dominated by metal orbital overlap with the C_2O_4 oxygen lone-pair orbitals (which favor α = 0.0°); the relatively weak Ti–O interactions involving the C_2O_4 π orbitals presumably account for the small folding angles (α = 11.4°). Both the cis and trans isomers of **2** have virtually identical MO correlation diagrams and similar MO compositions; thus, the Fenske-Hall model does not account for the solid-state occurrence of the cis isomer. The different redox properties of **1** and **2** were analyzed from considerations of the HOMO/LUMO compositions.

Introduction

In 1982 two reports[2,3] revealed that transition-metal species can reductively activate CS_2 to form a $S_2C\text{–}CS_2$ bond through an end-on bis(bimetallo-dithio) chelation,[2] which gave $[Fe_2(CO)_6]_2(C_2S_4)$, or a side-on bis(metallo-dithio) chelation,[3] which produced $[(\eta^5\text{-}C_5Me_5)Ni]_2(\mu\text{-}C_2S_4)$. Subsequent efforts to obtain other tetrathiolato (or tetrathiooxalato) transition-metal complexes by metal-promoted head-to-head reductive dimerization of CS_2[4,6,7] and CSe_2[5] have met with limited success.[4-9] Prior to our recent report,[10] all of this work involved the use of *late* transition metals (viz., Fe,[2,4] Co,[4] Ni,[3], Rh,[5-7], Ir[7]). Interest in developing this synthetic route to new transition-metal tetrathiolates and investigating their structural and physical-chemical properties was

---

[1] (a) Based in part on the Ph.D. thesis of H.A.H. at the University of Wisconsin, Jan 1988. Present address: Department of Chemistry, Creighton University, Omaha, NE 68178. (b) Present address: Department of Chemistry, Northwestern University, Evanston, IL 60201.

[2] $[Fe_2(CO)_6]_2(C_2S_4)$: Broadhurst, P. V.; Johnson, B. F. G.; Lewis, J.; Raithby, P. R. *J. Chem. Soc., Chem. Commun.* **1982**, 140–141.

[3] $[(\eta^5\text{-}C_5Me_5)Ni]_2(\mu\text{-}C_2S_4)$: Maj, J. J.; Rae, A. D.; Dahl, L. F. *J. Am. Chem. Soc.* **1982**, *104*, 4278–4280.

[4] $[(\eta^5\text{-}C_5Me_5)Co]_2(\mu\text{-}C_2S_4)$ and *trans*-$[(\eta^5\text{-}C_5Me_5)Fe(CO)]_2(\mu\text{-}C_2S_4)$: (a) Englert, M. H.; Maj, J. J.; Rae, A. D.; Jordan, K. T.; Harris, H. A.; Dahl, L. F. *Abstracts of Papers*, 187th National Meeting of the American Chemical Society, St. Louis, MO, Spring 1984; American Chemical Society: Washington, DC, 1984; INOR 280. (b) Englert, M. Ph.D. Dissertation, University of Wisconsin—Madison, 1983.

[5] $[(triphos)Rh)_2(\mu\text{-}C_2Se_4)]^{2+}$ (triphos = $MeC(CH_2PPh_2)_3$): Bianchini, C.; Mealli, C.; Meli, A.; Sabat, M. *J. Chem. Soc., Chem. Commun.* **1984**, 1647–1649.

[6] $[(triphos)Rh)_2(\mu\text{-}C_2S_4)]^{2+}$: Bianchini, C.; Mealli, C.; Meli, A.; Sabat, M. *Inorg. Chem.* **1984**, *23*, 4125–4127.

[7] $[(triphos)M)_2(\mu\text{-}C_2X_4)]^{2+}$ (M = Rh, X = S, Se; M = Ir, X = S): Bianchini, C.; Mealli, C.; Meli, A.; Sabat, M.; Zanello, P. *J. Am. Chem. Soc.* **1987**, *109*, 185–198.

[8] Bianchini, C.; Mealli, C.; Meli, A.; Sabat, M. In *Stereochemistry of Organometallic and Inorganic Compounds*; Bernal, I., Ed.; Elsevier: Amsterdam, 1986; pp 146–254.

[9] Touchard, D.; Fillaut, J.-L.; Khasnis, D. V.; Dixneuf, P. H.; Mealli, C.; Masi, D.; Toupet, L. *Organometallics*, **1988**, *7*, 67–75.

[10] $(Cp_2Ti)_2(\mu\text{-}C_2S_4)$: (a) Harris, H. A.; Rae, A. D.; Dahl, L. F. *J. Am. Chem. Soc.* **1987**, *109*, 4739–4741. (b) Harris, H. A. Ph.D. Dissertation, University of Wisconsin—Madison, 1988.

0002-7863/91/1513-8602$02.50/0 © 1991 American Chemical Society

partly motivated by difficulties encountered in obtaining tetrathiooxalate salts by chemical and electrochemical dimerization of CS_2.[11] The potential for transition-metal tetrathiolates to form a variety of one- and two-dimensional systems with metallic or semiconducting behavior[12] has been partially realized with the isolation of extended homo- and heterometallic complexes[11b,13] including highly conducting linear oligomers of $[M(C_2S_4)]_x$ (M = Ni, Cu, Pd).[14]

We recently reported the designed synthesis and characterization of $(Cp_2Ti)_2(\mu\text{-}C_2S_4)$ (**1**),[10] the first compound to be isolated as a result of an *early*-transition-metal-promoted dimerization of CS_2. This research was inspired by the discovery in 1981 by Floriani and co-workers[15] that reductive C–C coupling of *p*-tolylcarbodiimide, $C(NR)_2$, occurs upon its reaction with d^2 Ti(II) $Cp_2Ti(CO)_2$ to give $(Cp_2Ti)_2(\mu\text{-}C_2(NR)_4)$ (R = *p*-MeC_6H_4) (**3**). The magnetic, electrochemical, and geometrical properties of the C_2S_4-bridged **1** were found to differ markedly from those of the electronically equivalent oxalate-bridged $(Cp_2Ti)_2(\mu\text{-}C_2O_4)$ (**2**)[16,17] and tetra-*p*-tolyloxalilamidine-bridged $(Cp_2Ti)_2(\mu\text{-}C_2(NR)_4)$ (**3**).[15] That **1** is diamagnetic was conclusively established from a solid-state magnetic susceptibility measurement at room temperature in accordance with its relatively sharp ^1H NMR signal and the absence of any observable EPR signal in solution at room temperature or in a THF glass at −105 °C. In contrast, both **2** and **3** are paramagnetic with two unpaired electrons at room temperature.[15,17] Variable-temperature magnetic susceptibility measurements of **2** down to 4.2 K showed that the effective magnetic moment per titanium is independent of temperature and corresponds to a spin-only value from room temperature down to ~130 K, below which the moment per titanium decreases to 1.33 μ_B at 4.2 K. These results were quantitatively analyzed by Hendrickson, Stucky, and co-workers[17] as a weak antiferromagnetic exchange interaction, which is completely consistent with the magnetic separation of two d^1 Ti(III) Cp_2Ti^+ fragments by a tetradentate $C_2X_4^{2-}$ ligand (X = O, NR) such that the singlet–triplet energy gap is small. A cyclic voltammogram of **1** in either CH_2Cl_2 or THF displays two quasi-reversible one-electron reductions and no oxidations, whereas both **2** and **3** can be oxidized in a single step to the corresponding dications. These electrochemical data led to the proposal[10] that oxidation to give the d^0 Ti(IV) dications occurs in **2** and **3** (but not in **1**) because the electrons removed are predominantly metal-localized in **2** and **3**.

The major differences between the molecular geometry of **1** and those of **2**[16] and **3**[15] were also interpreted[10] in terms of much greater electron delocalization of the C_2X_4-bridged ligand in **1**. The C–C bond distances of 1.523 (11) Å in **2** and 1.504 (6) Å in **3** approximately conform to single-bond values in harmony with the C_2X_4 ligand (X = O, NR) being considered as a dianion. In contrast, the C–C bond distances in the four crystallographically independent half-molecules of **1** have a significantly shorter mean value of 1.41 Å (range 1.40 (2)–1.42 (2) Å), which is still considerably longer than that of 1.34 Å for a normal C–C double bond. This bond-length difference coupled with the tilt of each of the two TiX_2 planes out of the $X_2C_2X_2$ plane by 46.5° in **1** vs only 11.4° in **2** and 11.1° in **3** gave rise to the hypothesis[10] that whereas **2** and **3** possess electron-localized configurations involving the interaction of a $C_2O_4^{2-}$ or $C_2(NR)_4^{2-}$ dianion with two d^1 Ti(III) Cp_2Ti^+ fragments, **1** has an electron-delocalized configuration in which the C_2S_4 ligand can be regarded (from a valence-bond viewpoint) as an intermediate between a tetrathiooxalate dianion and an ethylenetetrathiolate tetraanion.

The nature of the bridging C_2S_4 ligand in the *late*-transition-metal systems that have been studied in the past is still not settled. From an extensive MO examination via the extended Hückel model on both side-on and end-on chelate linkages of various metal fragments with C_2S_4-bridged ligands, Alvarez, Vicente, and Hoffmann[12] stated that the description of the C_2S_4 ligand as dianionic or tetraanionic is not easy and depends upon the particular complex. On the basis of a comprehensive experimental and theoretical investigation of C_2S_4- and C_2Se_4-bridged dimetal dications of formula $[((triphos)M)_2(\mu\text{-}C_2X_4)]^{2+}$ (M = Rh, X = S, Se; M = Ir, X = S; triphos = $MeC(CH_2PPh_2)_3$), Bianchini et al.[6,7] concluded from extended Hückel calculations that the C_2X_4-bridged ligand may be described as a dianion. They[7] also analyzed the formation of the C_2X_4-bridged ligand from the C–C coupling of the two η^2-coordinated CS_2 ligands. From MO studies via the Fenske–Hall model[18] on the $(Cp^*M)_2(\mu\text{-}C_2S_4)$ (M = Ni, Co, *trans*-Fe(CO); Cp* = $\eta^5\text{-}C_5Me_5$), Englert et al.[4] concluded that the geometrical variations among these tetrathiolene-like dimetal complexes are consistent with the MO calculations pointing to a significant difference in electron delocalization such that integral oxidation states were not assigned to the bridging C_2S_4 ligand and the metal atoms.

In order to obtain a more quantitative assessment of the apparent electron delocalization observed for the *early*-transition-metal tetrathiolate-bridged **1** and to more fully understand how this molecule theoretically interrelates with the electron-localized C_2O_4-bridged analogue, a molecular orbital study was undertaken with the Fenske–Hall model.[18] The results of this study are presented here.

Molecular orbital calculations were performed on two $[(Cp_2M)_2(\mu\text{-}C_2X_4)]^n$ series: (a) M = Ti, X = S, *n* = 2+, 0, 1−, 2−; (b) M = Ti, X = O, *n* = 2+, 0, 2−. Additionally, the equilibrium geometries of the individual members of these two series were varied (i.e., specifically, the degree to which the Cp_2Ti fragments are displaced from the plane of the C_2X_4 ligand) so as to determine the effects of geometrical change on the electronic structure of the molecules. A comparative bonding analysis of these two series is presented, and theoretical explanations for the observed experimental differences are given.

Computational Details

Fenske–Hall MO Method. Molecular orbital calculations were carried out on a VAX 8650 computer system with the Fenske–Hall molecular orbital model.[18] This model is based on a self-consistent field (SCF) method, which is an approximation of the Hartree–Fock–Roothaan procedure. The model is devoid of adjustable or empirical parameters such that the resulting eigenvectors and eigenvalues from a calculation are completely determined by the input geometry and by the nature and size of the basis functions. A detailed discussion of this method and examples of its utility are presented elsewhere.[19,20]

Population Analyses. In this work we utilized natural atomic populations as well as the more familiar, yet perpetually criticized Mulliken atomic populations. The natural populations were computed with the natural bond orbital (NBO) algorithm[21,22] developed by Weinhold and co-workers.[23] The NBO procedure performs a modified Löwdin sym-

---

(11) (a) Tetraalkylammonium salts of the tetrathiooxalate dianion (C_2S_4), which is unstable in air, can be prepared by the electrochemical reduction of CS_2 in MeCN saturated with R_4NBr: Jeroschewski, P. *Z. Chem.* **1981**, *21*, 412. (b) Hoyer, E. *Comments Inorg. Chem.* **1983**, *2*, 261–270, and references cited therein.

(12) Alvarez, S.; Vicente, R.; Hoffmann, R. *J. Am. Chem. Soc.* **1985**, *107*, 6253–6277, and references therein.

(13) (a) Poleschner, H.; John, W.; Kempe, G.; Hoyer, E.; Fanghanel, E. *Z. Chem.* **1978**, *18*, 345–346. (b) Strauch, P.; Dietzsch, W.; Hoyer, E. *Z. Chem.* **1983**, *23*, 448–449.

(14) Reynolds, J. R.; Karasz, F. E.; Lillya, C. P.; Chien, J. C. W. *J. Chem. Soc., Chem. Commun.* **1985**, 268–269.

(15) $(Cp_2Ti)_2(\mu\text{-}C_2(NR)_4)$ (R = *p*-MeC_6H_4): Pasquali, M.; Floriani, C.; Chiesi-Villa, A.; Guastini, C. *Inorg. Chem.* **1981**, *20*, 349–355.

(16) $(Cp_2Ti)_2(\mu\text{-}C_2O_4)$: Bottomley, F.; Lin, I. J. B.; White, P. S. *J. Organomet. Chem.* **1981**, *212*, 341–349; *Ibid.* **1982**, *232*, C19.

(17) $(Cp_2Ti)_2(\mu\text{-}C_2O_4)$: Francesconi, L. C.; Corbin, D. R.; Clauss, A. W.; Hendrickson, D. N.; Stucky, G. D. *Inorg. Chem.* **1981**, *20*, 2059–2069.

(18) Hall, M. B.; Fenske, R. F. *Inorg. Chem.* **1972**, *11*, 768–775.

(19) (a) Fenske, R. F. *Prog. Inorg. Chem.* **1976**, *21*, 179–208. (b) Fenske, R. F. *Pure Appl. Chem.* **1971**, *27*, 61–71.

(20) Kanis, D. R. Ph.D. Thesis, University of Wisconson—Madison, 1988.

(21) The general version of the natural bond orbital procedure, GENNBO, which was altered (by D.R.K.) in order to accommodate the many atoms and their basis functions involved in these calculations, utilized the Fock, overlap, and bond order matrices from the Fenske–Hall MO calculations. A special version of the Fenske–Hall program, NBOMED,[20] supplied the necessary data in proper format to GENNBO.[22]

(22) A version of the natural bond orbital program suitable for general usage is available from the Quantum Chemistry Exchange Program, Indiana University, Bloomington, IN: Reed, A. E.; Weinhold, F. *QCPE Bull.* **1985**, *5*, 141.

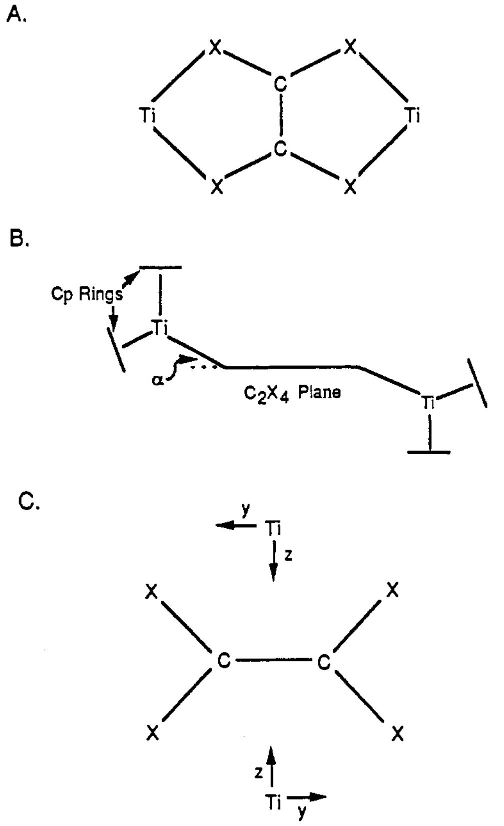

Figure 1. Geometry of $(Cp_2Ti)_2(\mu\text{-}C_2X_4)$ (X = S (**1**), O (**2**)): (a) view of the $TiX_2C_2X_2Ti$ core; (b) view parallel to the C_2X_4 ligand plane showing the folding of one TiX_2 plane by angle α with respect to the C_2X_4 plane; (c) coordinate systems for the Ti atoms relative to the bridging ligand. A right-handed coordinate system is used.

metric orthogonalization[24] on a Fenske–Hall wave function in order to construct a new set of basis functions, the so-called natural atomic orbitals, which are orthogonal to those on different atomic centers.[25] Conventional basis functions are constructed to be orthogonal to functions on the *same* center but are not orthogonal to functions on *different* centers. By virtue of this orthogonalization of basis functions between centers, a natural atomic charge analysis circumvents the partitioning problem inherent in the Mulliken scheme.[26] A Mulliken analysis dictates equal (democratic) partitioning of shared electron density, clearly an incorrect prescription. The partitioning problem is particularly evident in the results of the Fenske-Hall model applied to **1** and **2** in that the comparative theoretical analysis involves C_2X_4 ligands with widely different electronegative X atoms. Valence s and p metal functions are allocated far too much electron density. As a consequence, metal charges are too negative, while ligand charges are often underestimated. Since the natural populations are not dependent upon a "partitioning bias", they provide a more realistic analysis of the atomic charges in **1** and **2**.

Basis Functions. Clementi's free-atom double-ζ Hartree–Fock functions[27] were used for C, O, and S. All but the valence-shell p functions were curve-fit to single-ζ form by use of the criterion of maximum overlap.[28] A value of 1.16 was used for the H 1s atomic orbital.[29] The titanium 1s through 3d atomic orbital functions were taken from Richardson et al.[30] The exponents for the single-ζ titanium 4s and 4p orbitals were set at 1.8 and 1.6, respectively.

Table I. Bond Lengths and Angles Used in the Idealized Geometries of $(Cp_2Ti)_2(\mu\text{-}C_2X_4)$ (X = S (**1**), O (**2**))

A. Bond Lengths (Å)

compound	Ti–X	X–C	C–C	Ti–C (ring)
$(Cp_2Ti)_2(\mu\text{-}C_2S_4)$	2.407	1.736	1.411	2.383
$(Cp_2Ti)_2(\mu\text{-}C_2O_4)$	2.158	1.256	1.523	2.451

B. Bond Angles (deg)

compound	X–Ti–X	Ti–X–C	X–C–C	X–C–X	Cp–Ti–Cp[a]
$(Cp_2Ti)_2(\mu\text{-}C_2S_4)$	81.6	97.1	120.0	120.0	133.7
$(Cp_2Ti)_2(\mu\text{-}C_2O_4)$	75.8	114.5	116.7	126.6	125.4

[a] Cp denotes the centroid of a cyclopentadienyl ring.

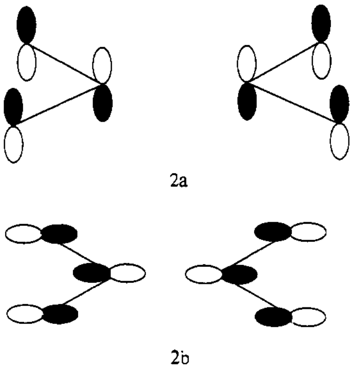

Figure 2. Crucial orbitals in the reductive dimerization of $C_2X_4^{2-}$ from CX_2: (a) coupling interaction that forms the $C_2X_4^{2-}$ π-acceptor LUMO; (b) coupling interaction between two singly occupied orbitals in CX_2^- resulting in a carbon–carbon σ bond.

Geometries. Molecular geometries for $(Cp_2Ti)_2(\mu\text{-}C_2X_4)$ (X = S, O) are based upon X-ray crystal structure data.[10,16] Mean bond distances and angles are given in Table I. The trans configuration (α = 46.5°) of the C_2S_4-bridged **1**, which has crystallographic C_i-$\bar{1}$ site symmetry, was idealized to C_{2h}-$2/m$ symmetry with the principal C_2 axis along the C–C bond. The cis configuration (α = 11.4°) of the C_2O_4-bridged **2**, which has a crystallographic 2-fold axis perpendicular to the C_2O_4 ligand and passing through the center of the C–C bond, was idealized to C_{2v}-$2mm$ symmetry. Calculations were also carried out on the hypothetical trans isomer (α = 11.4°) of **2**.

General Considerations. Local right-handed orthogonal coordinate systems of the titanium atoms relative to the positions of the atoms in the bridging ligand are shown in Figure 1c. In each series the origin of the right-handed master coordinate system was chosen to be at the center of the bridging C–C bond. The C_2X_4 ligand lies in the Y–Z plane of the master coordinate system with the Z axis along the C–C bond and with the Y axis bisecting the four sulfur or oxygen atoms. Each titanium atom lies within the X–Y plane (its Z coordinate is zero). The local coordinate systems for the ligand atoms are such that the z axis of each of the two central carbon atoms points at the origin of the master coordinate system, the z axis of each bridging sulfur or oxygen atom points to the carbon atom to which it is bonded, the z axis of each Ti atom points to the midpoint of the two sulfur or oxygen atoms to which it is bonded, and the z axis of each carbon atom in a Cp ring points to the centroid of the ring.

Each of the C_2X_4-bridged dititanium complexes was divided into seven fragments: four Cp rings, one bridging C_2X_4 unit, and the two titanium atoms. Calculations were first carried out on the non-metal fragments and then on the composite molecule. The eigenvectors resulting from calculations of the "free" Cp^- anion and "free" $C_2X_4^{2-}$ dianion were used as basis sets for these ligands when the calculation was done on the entire molecule. The low-lying occupied σ orbitals of each ligand (viz., the five C–C and five C–H σ-bonding orbitals for each Cp ring and five C–C and C–X σ-bonding orbitals for the C_2X_4 unit) were frozen as ligand core orbitals and thereby were deleted (along with the virtual σ-antibonding valence ligand orbitals) from the SCF procedure.[31,32] This treatment,

---

(23) (a) Foster, J. P.; Weinhold, F. *J. Am. Chem. Soc.* **1980**, *102*, 7211–7218. (b) Rives, A. B.; Weinhold, F. *Int. J. Quantum Chem., Symp.* **1980**, *14*, 201–209; *Ibid.* **1981**, *15*, 555. (c) Reed, A. E.; Weinstock, R. B.; Weinhold, F. *J. Chem. Phys.* **1985**, *83*, 735–746. (d) Reed, A. E.; Curtiss, L. A.; Weinhold, F. *Chem. Rev.* **1988**, *88*, 899–926.

(24) (a) Löwdin, P.-O. *J. Chem. Phys.* **1950**, *18*, 365–375. (b) Löwdin, P.-O. *Adv. Quantum Chem.* **1970**, *5*, 185–199.

(25) Reed, A. E.; Weinhold, F. *J. Chem. Phys.* **1983**, *78*, 4066–4073.

(26) (a) Mulliken, R. S. *J. Chim. Phys. Phys. Chim. Biol.* **1949**, *46*, 500–542. (b) Löwdin, P.-O. *J. Chem. Phys.* **1953**, *21*, 374–375. (c) Mulliken, R. S. *J. Chem. Phys.* **1955**, *23*, 1841–1846.

(27) Clementi, E.; Ramondi, D. L. *J. Chem. Phys.* **1963**, *38*, 2686–2689.

(28) Radtke, D. D. Ph.D. Dissertation, University of Wisconsin—Madison, 1966.

(29) Hehre, W. J.; Stewart, R. F.; Pople, J. A. *J. Chem. Phys.* **1969**, *51*, 2657–2664.

(30) Richardson, J. W.; Nieuwport, W. C.; Powell, R. R.; Edgell, W. F. *J. Chem. Phys.* **1962**, *36*, 1057–1061.

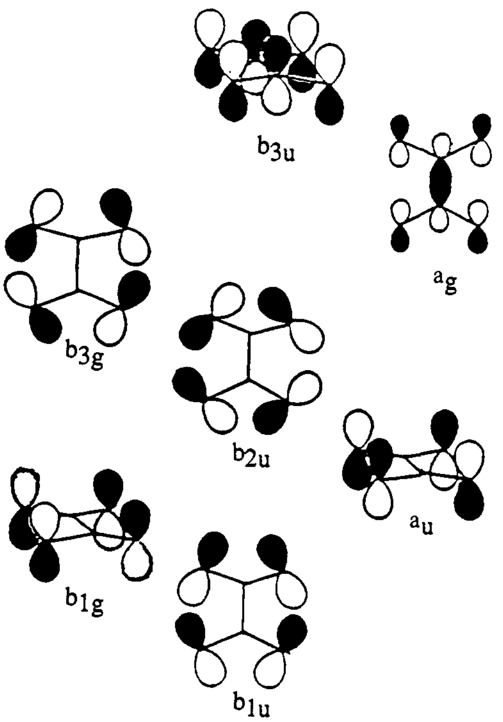

Figure 3. Molecular orbitals for $C_2X_4^{2-}$ labeled under D_{2h} symmetry.

Table II. Energies and Percent Compositions of Molecular Orbitals of $C_2X_4^{2-}$ under D_{2h} Symmetry

	energy (eV)		% C orbital[b] character	
MO	X = O	X = S	X = O	X = S
b_{1u}	−17.0	−11.2	6.24	3.68
b_{1g}	−15.8	−11.6	0.00	0.00
a_u	−15.7	−10.8	0.00	0.00
b_{2u}	−15.3	−11.3	0.00	0.00
b_{3g}	−14.7	−8.5 (H)[a]	0.12	0.54
a_g	−11.6 (H)[a]	−11.5	8.88	4.82
b_{3u}	−4.3 (L)[a]	−6.8 (L)[a]	43.90	31.60

[a] H and L denote the HOMO and LUMO, respectively. [b] The percentage is summed over both carbon atoms in the "free" $C_2X_4^{2-}$ ligand.

which avoids possible counterintuitive orbital mixing,[33] is identical to that performed by others[34,35] on first-row transition-metal cyclopentadienyl complexes. Lichtenberger and Fenske[35] found that this procedure substantially reduced the time for solution of the SCF equations without introducing serious errors into the results. Calculations were performed for both **1** and **2** with each cyclopentadienyl ligand treated as a monoanion (closed shell) and with the $C_2X_4^{n-}$ ligand formulated as a dianion in order to be consistent with a formal oxidation state of III for each titanium atom. Petersen et al.[34] found in their Fenske–Hall MO analysis of Cp_2ML_2 complexes (M = Ti, V; L_2 = S_5, Cl_2) that treating the cyclopentadienyl ligand as a radical (open shell) or as a monoanion (closed shell) did not significantly affect the orbital character. The transformation of the ligand basis set from atomic orbitals to molecular "fragment" orbitals does not affect the numerical results of the calculation but does allow for an easier interpretation of the bonding scheme in the molecular complex. The energies of the ligand MOs in the correlation diagrams are diagonal elements of the Fock matrices obtained from the calculations on the entire complex.

Results and Discussion

Analysis of the Molecular Fragment Ligands. (a) Cp Ligand. The electronic structure of the "free" cyclopentadienyl monoanion is well-known[35,36] and will not be detailed here. The important π orbitals for η^5 coordination to a transition metal are the filled a_2 and e_1 orbitals (under D_{5h} symmetry); the latter orbitals constitute the degenerate HOMOs for the free Cp anion.

(b) $C_2X_4^{2-}$ Ligand. The differences in the magnetic and electrochemical properties of $(Cp_2Ti)_2(\mu\text{-}C_2S_4)$ (**1**) and $(Cp_2Ti)_2(\mu\text{-}C_2O_4)$ (**2**) can be directly attributed to the significant variations in character of the corresponding frontier orbitals arising from the formal substitution of the less electronegative sulfur atoms for the oxygen atoms in the bridging ligands. Thus, it is worthwhile to examine the electronic structure of each $C_2X_4^{2-}$ fragment.

The formation of a symmetric $C_2X_4^{2-}$ dianion from the reductive coupling of two linear CX_2 molecules has been described by Gimarc[37] and subsequently by Alvarez, Vicente, and Hoffmann.[12] These contributions discuss the electronic consequences of transforming CX_2 from a linear geometry ($D_{\infty h}$ symmetry) into the atomic arrangement required for reductive dimerization to $C_2X_4^{2-}$ (bent C_{2v} symmetry). In this framework, the electronic differences between $C_2O_4^{2-}$ and $C_2S_4^{2-}$ are easily delineated.

Gimarc[37] predicted in 1979, on the basis of perturbation theory and electronegativity arguments, that the C–C bond in $C_2S_4^{2-}$ would be weaker than the C–C bond in $C_2O_4^{2-}$. The results of Fenske–Hall calculations on the "free" $C_2X_4^{2-}$ dianions (with assumed planar D_{2h} geometries) clearly show that the differences in electronegativity between carbon, sulfur, and oxygen are important, but not for the reasons that Gimarc gave.

The lowest unoccupied molecular orbitals in both CO_2 and CS_2 are the doubly degenerate π_u* orbitals. One of these LUMOs, which is stabilized relative to the other (see Figure 2) upon transformation to C_{2v} symmetry, formally gains one electron upon reduction to CX_2^-. As displayed in Figure 2b, this orbital is now in position to couple with its counterpart in another CX_2^- moiety to form the carbon–carbon σ bond present in the dianion. This simple reductive dimerization scheme accurately describes the formation of $C_2O_4^{2-}$ from CO_2^-; however, the description of the dithiolate system is a bit more complicated. The "coupling" orbital in the CS_2^- dimerization is in the energetic proximity of an orbital

---

(31) It has been suggested to us by one reviewer that in "freezing out" the ligand σ framework (the five σ bonds) from the variational procedure, we may also be deleting important anomeric ("negative" hyperconjugation) electronic effects. Since the anomeric effect is much more pronounced in carbon molecules involving first-row heteroatoms relative to those involving corresponding second-row heteroatoms,[32] the σ frameworks in the $C_2X_4^{2-}$ ligands may well play a role in distinguishing "free" $C_2O_4^{2-}$ from "free" $C_2S_4^{2-}$ and $(Cp_2Ti)_2(\mu\text{-}C_2O_4)$ from $(Cp_2Ti)_2(\mu\text{-}C_2S_4)$. Specifically, the interaction between oxygen lone pairs and the *vicinal* antiperiplanar C–C σ* function should be much greater in the oxalate dianion than the analogous interaction in the tetrathiooxalate dianion according to the current understanding of the anomeric effect. To determine the relative significance of the anomeric effect in the $C_2X_4^{2-}$ species, we performed MO computations on the actual $C_2S_4^{2-}$ structure and a hypothetical structure of $C_2O_4^{2-}$ where the C–C distance was set equal to that in the $C_2S_4^{2-}$ species. With use of an integrated Fenske–Hall/natural bond orbital approach,[20,21] the computed occupations of the C–C σ* bonds are 0.054 in the oxalate and 0.025 in the tetrathiooxalate dianion. From our calculations, we conclude that the anomeric effect is, in fact, much more significant for the oxalate dianion than the tetrathiooxalate dianion and could be responsible for the difference in C-C bond lengths in the free moieties. However, since we included all the valence orbitals when computing the electronic structure of the free ligand, our computations will account for this anomeric effect. The validity of neglecting the $C_2X_4^{2-}$ σ framework interactions with the titanium fragments in the energy minimization of the dititanium species will rest on the change in C–C σ* population upon complexation to the titanium fragments. Our Fenske–Hall/NBO procedure revealed that there is only a nominal change in the carbon–carbon antibonding orbital population when the σ framework is allowed to interact versus when it is not allowed to interact with the $TiCp_2$ fragments (viz., 0.029 vs 0.027 in **1** and 0.072 vs 0.072 in **2**). For the sake of completeness we also compared the $(Cp_2Ti)_2(\mu\text{-}C_2X_4)$ orbital eigenvectors and eigenvalues with and without the inclusion of the $C_2X_4^{2-}$ σ framework. We found that the computed orbital eigenvalues were in agreement to within 1% and that the eigenvectors were basically identical with the exception of the very low-lying molecular orbitals where counterintuitive molecular orbital mixing[33] is prominent. On the basis of these observations, we conclude that the anomeric effect is *not* responsible for the contrasting electrochemical, structural, and magnetic properties observed in **1** and **2**.

(32) Schleyer, P. v. R.; Jemmis, E. D.; Spitznagel, G. W. *J. Am. Chem. Soc.* **1985**, *107*, 6393–6394, and references therein.

(33) Whangbo, M. H.; Hoffmann, R. *J. Chem. Phys.* **1978**, *68*, 5498–5500.

(34) Petersen, J. L.; Lichtenberger, D. L.; Fenske, R. F.; Dahl, L. F. *J. Am. Chem. Soc.* **1975**, *97*, 6433–6441.

(35) (a) Lichtenberger, D. L.; Fenske, R. F. *J. Am. Chem. Soc.* **1976**, *98*, 50–63. (b) Lichtenberger, D. L.; Fenske, R. F. *J. Chem. Phys.* **1976**, *64*, 4247–4264. (c) Lichtenberger, D. L.; Fenske, R. F. *Inorg. Chem.* **1976**, *15*, 2015–2022.

(36) See for example, Cotton, F. A. *Chemical Applications of Group Theory*; Wiley: New York, 1971; p 142.

(37) Gimarc, B. M. *Molecular Structure and Bonding*; Academic Press: New York, 1979; pp 187–192.

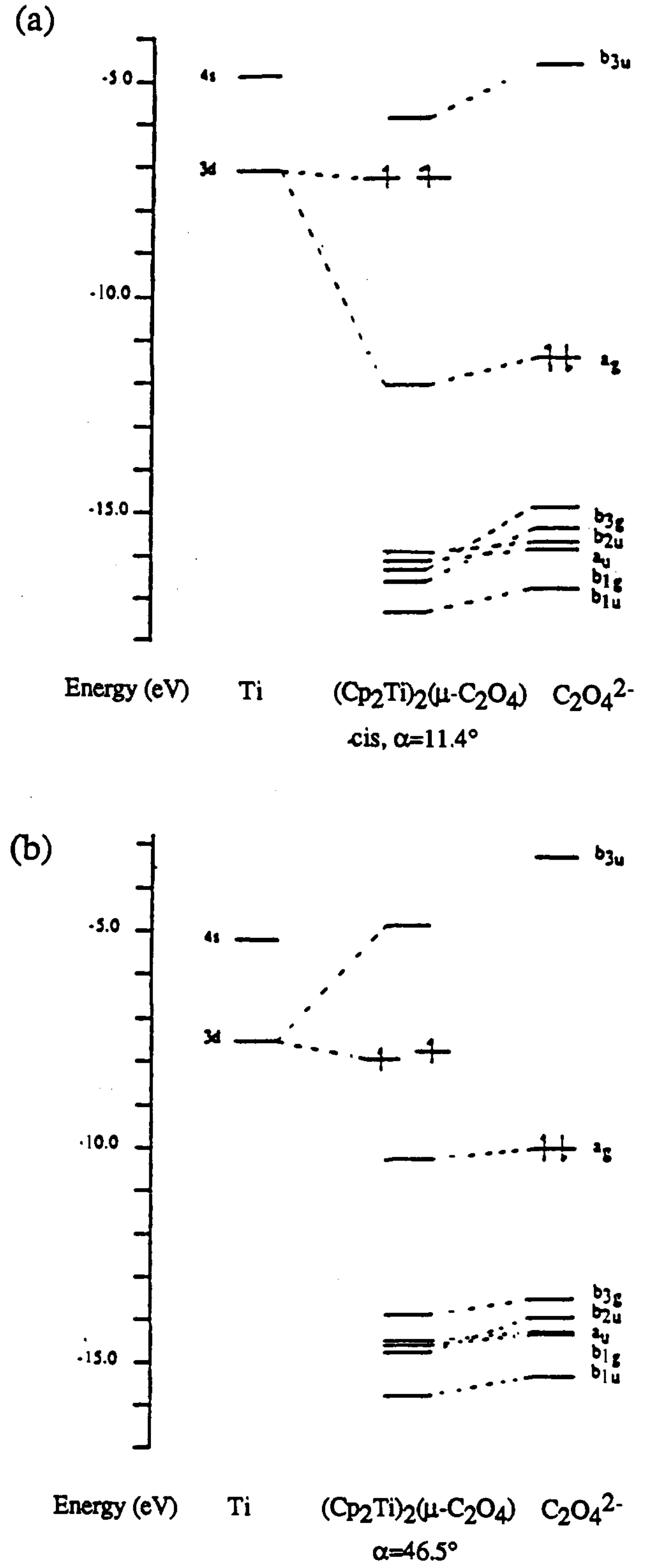

Figure 4. MO correlation diagrams for $(Cp_2Ti)_2(\mu\text{-}C_2O_4)$: (a) cis isomer, α = 11.4° and trans isomer, α = 11.4°; (b) trans isomer, α = 46.5°.

with the same symmetry (a_1 in C_{2v} molecular symmetry); thus, substantial orbital mixing stabilizes the "coupling" interaction in the dithiolate dianion relative to that in the oxalate dianion. As shown in Table II, our calculations reveal that the C–C coupling orbital (labeled a_g in Figures 4 and 5 and in Table II) is the HOMO in $C_2O_4^{2-}$; however, its counterpart lies far below the HOMO in $C_2S_4^{2-}$ by virtue of this stabilizing interaction.

Using similar arguments, one can rationalize the relative energetics of the LUMOs (labeled as b_{3u} in Figures 4 and 5 and in Table II) of the two dianions. Unoccupied π orbitals in two

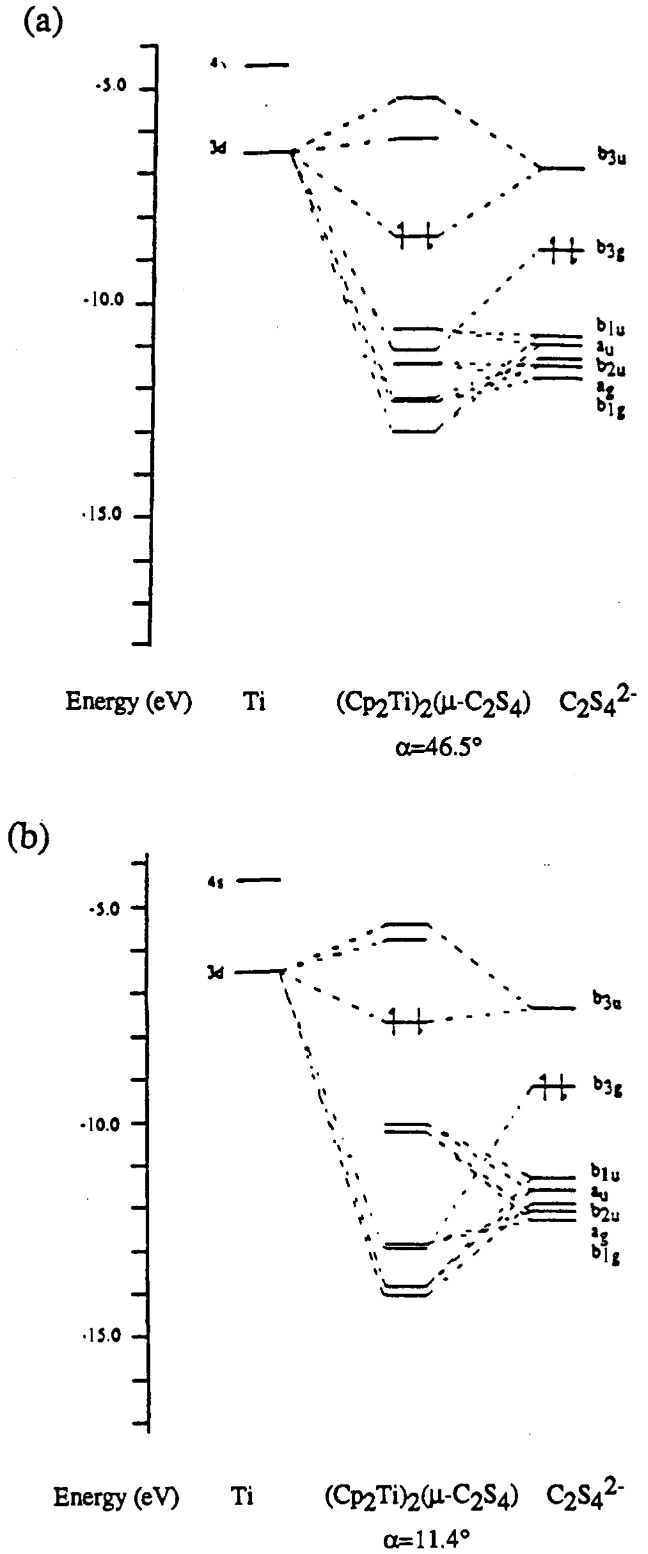

Figure 5. MO correlation diagrams for $(Cp_2Ti)_2(\mu\text{-}C_2S_4)$: (a) trans isomer, α = 46.5°; (b) trans isomer, α = 11.4°.

CX_2^- fragments (see Figure 2a) combine to form the LUMOs in both dianions. Once again, an orbital of the correct symmetry is energetically accessible to the $C_2S_4^{2-}$ function. However, the energetic disparity between analogous orbitals in the oxalate fragment attenuates the imparted "stabilization" of the LUMO. Therefore, the LUMO of $C_2S_4^{2-}$ (at −6.8 eV) is "stabilized" relative to that in $C_2O_4^{2-}$ (at −4.3 eV). We will demonstrate that the 2.5-eV stabilization of the $C_2S_4^{2-}$ LUMO relative to its $C_2O_4^{2-}$ counterpart is responsible for the contrasting magnetic, electrochemical, and structural properties of the electronically equivalent $(Cp_2Ti)_2(\mu\text{-}C_2O_4)$ and $(Cp_2Ti)_2(\mu\text{-}C_2S_4)$ molecules.

Table III. Energy and Percent Composition of Selected Molecular Orbitals for Cis and Trans Isomers of $(Cp_2Ti)_2(\mu\text{-}C_2X_4)$ (**1**, X = S; **2**, X = O)

molecule	orbital	energy (eV)	% Ti	% C_2X_4	% Cp^a
2: trans, $\alpha = 11.4°$	$HOMO^b$	−7.27	89.9	3.8	6.3
	HOMO	−7.17	89.6	4.8	5.6
	LUMO	−5.83	68.4	19.1	12.5
2: cis, $\alpha = 11.4°$	HOMO	−7.34	87.9	5.3	6.8
	HOMO	−7.11	92.1	0.9	7.0
	LUMO	−5.79	69.6	17.6	12.8
2: trans, $\alpha = 46.5°$	HOMO	−7.98	87.1	5.9	7.0
	HOMO	−7.82	90.8	3.5	5.7
	LUMO	−5.93	83.9	1.7	14.4
2: trans, $\alpha = 0.0°$	HOMO	−7.23	90.3	2.8	6.9
	HOMO	−7.07	91.2	0.9	7.9
	LUMO	−5.83	63.6	23.2	13.2
1: trans, $\alpha = 46.5°$	HOMO	−8.47	34.5	59.9	5.6
	LUMO	−6.15	81.3	9.3	9.4
1: trans, $\alpha = 11.4°$	HOMO	−7.66	21.1	63.5	15.4
	LUMO	−5.81	81.2	10.4	8.4

[a] The percentage is summed over all four Cp rings of each molecule. [b] The two HOMOs for each oxalate-bridged molecule are singly occupied.

The calculations indicate no significant difference between the overlap populations of the carbon $2p_z$ and 2s orbitals that are responsible for the formation of the C–C σ bond in the dianions (0.76 for X = O vs 0.77 for X = S). The total overlap population, however, is significantly greater for X = S (1.10) than for X = O (0.96) due to an increased population of the C $2p_x$ orbitals, which give delocalized π character to the (planar) system. In the oxalate system the larger electronegativity of oxygen relative to that of carbon localizes the electron density in oxygen lone-pair orbitals and in the C–O bonding orbitals rather than in the C–C bonding orbitals. These conclusions are consistent with the C–C bond length of 1.46 (2) Å reported[38] for the highly nonplanar $C_2S_4^{2-}$ dianion (SCCS torsional angle 79.5°) in a hydrated tetraphenylphosphonium salt. This bond length is shorter than the typical C–C single-bond length of 1.52–1.58-Å range found for the planar or nearly planar $C_2O_4^{2-}$ dianion in ionic and metal-chelated oxalate complexes.[39–43]

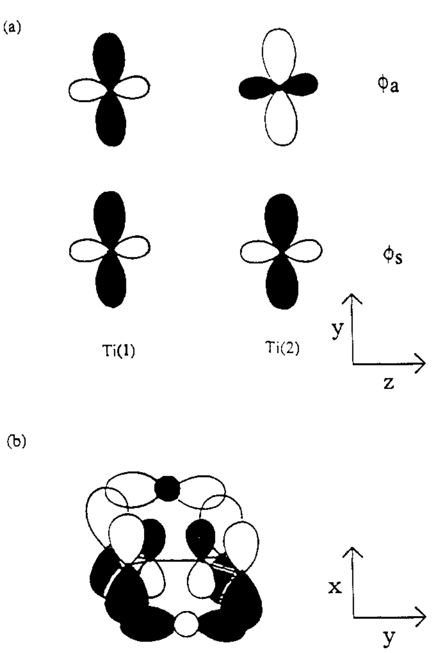

Figure 6. (a) Antisymmetrical (ϕ_a) and symmetrical (ϕ_s) dititanium combinations for the $3d_{x^2-y^2}/d_{z^2}$ Ti hybrid orbitals that form an accidentally degenerate set of half-occupied HOMOs in either the cis or trans isomer ($\alpha = 11.4°$) of **2**. (b) The nondegenerate filled HOMO (b_u under C_{2h} symmetry) formed in the trans isomer of **1** by the strong bonding interaction of the ϕ_a combination of the $3d_{x^2-y^2}/d_{z^2}$ Ti hybrid orbitals with the π-acceptor C_2S_4 orbital (b_{3u} under D_{2h} ligand symmetry). This nondegenerate HOMO results in spin pairing of the unpaired electron on each Ti in **1** by electron delocalization over the entire $TiS_2C_2S_2Ti$ core.

Molecular Orbital Analysis of $(Cp_2Ti)_2(\mu\text{-}C_2O_4)$. The experimentally determined geometry[16] of $(Cp_2Ti)_2(\mu\text{-}C_2O_4)$ possesses a nonplanar $TiO_2C_2O_2Ti$ core of C_{2v} symmetry in which each Ti atom is displaced out of the C_2O_4 plane in the same direction by ~0.3 Å. The extent of this cis folding along the two O--O vectors, which can be measured by the angle α that each TiO_2 plane makes with the C_2O_4 plane, is 11.4° for **2**. In the electronically equivalent $(Cp_2Ti)_2(\mu\text{-}C_2(NR)_4)$ (**3**), a C_{2h} trans folding of the same magnitude (11.1°) is observed.[15] For this reason, calculations were done on both cis and trans isomers of **2** (with $\alpha = 11.4°$) to determine if there is any electronic explanation for the occurrence of the two different isomers.

A comparison of frontier orbital eigenvectors and eigenvalues for the cis and trans isomers is given in Table III. The orbital eigenvalues for the two isomers are virtually identical, as are the compositions of the frontier orbitals. Not surprisingly, the molecular orbital correlation diagram of the trans isomer is a virtual duplicate of that for the cis isomer within the Fenske–Hall model (both MO diagrams are represented by Figure 4a). Our results suggest, therefore, that there are no significant electronic differences between the cis and trans configurations ($\alpha = 11.4°$) of $(Cp_2Ti)_2(\mu\text{-}C_2O_4)$.

As displayed in Figure 4a, there are six metal–ligand interactions in the dititanium oxalate species, all primarily ligand centered due to a large (>8 eV) energy gap between the higher

---

(38) $[PPh_4]^+_2[C_2S_4]^{2-}\cdot 6H_2O$: Lund, H.; Hoyer, E.; Hazell, R. G. *Acta Chem. Scand., Ser. B* **1982**, *B36*, 207–209.

(39) (a) $K_2(C_2O_4)\cdot H_2O$ (1.570 (2) Å): Sequeira, A.; Srikanta, S.; Chidambaram, R. *Acta Crystallogr., Sect. B* **1970**, *B26*, 77–80. (b) $K_2(C_2O_4)\cdot D_2O_2$ (1.565 (9) Å); $Rb_2(C_2O_4)\cdot D_2O_2$ (1.587 (7) Å): Adams, J. M.; Ramdas, V.; Hewat, A. W. *Acta Crystallogr., Sect. B* **1980**, *B36*, 570–574. (c) $(NH_4)^+_2(C_2O_4)^{2-}\cdot H_2O$ (1.565 (14) Å): Taylor, J. C.; Sabine, T. M. *Acta Crystallogr., Sect. B* **1972**, *B28*, 3340–3351. (d) $[C_{17}H_{24}N_4O]^{2+}(C_2O_4)^{2-}\cdot H_2C_2O_4$ (1.541 (11) Å): Van der Brempt, C.; Durant, F.; Norberg, B.; Evrard, G. *Acta Crystallogr. Sect. C: Cryst. Struct. Commun.* **1985**, *C41*, 1532–1535. (e) $Ca(C_2O_4)\cdot 3H_2O$ (1.557 (4) and 1.558 (3) Å): Blom, N. S.; Kanters, J. A.; Heijnen, W. M. M. *Cryst. Struct. Comm.* **1981**, *10*, 1283–1288. (f) $K_4[Zr(C_2O_4)_4]\cdot 5H_2O$ (1.535 (6)–1.550 (5) Å): Kojic-Prodic, B.; Ruzic-Toros, Z.; Sljukic, M. *Acta Crystallogr., Sect. B* **1978**, *B34*, 2001–2002. (g) $Cs^+[V(C_2O_4)_2(H_2O)_2]^-\cdot 4H_2O$ (1.547 (6) Å); $[MeNH_3]^+[V(C_2O_4)_2(H_2O)_2]^-\cdot 4.5H_2O$ (1.542 (12) Å): Grey, I. E.; Madsen, I. C.; Sirat, K.; Smith, P. W. *Acta Crystallogr., Sect. C: Cryst. Struct. Commun.* **1985**, *C41*, 681–683. (h) $[NH_4]^+[Al(C_2O_4)_3]^{3-}\cdot 3H_2O$ (1.545 (3)–1.552 (2) Å): Bulc, N.; Golic, L.; Siftar, J., *Acta Crystallogr., Sect. C: Cryst. Struct. Commun.* **1984**, *C40*, 1829–1831. (i) $[(C_{18}H_{34}N_6)Ni)_2(\mu\text{-}C_2O_4)]^{2+}[ClO_4]^-_2\cdot 2H_2O$ (1.531 (12) Å): Davis, A. R.; Einstein, W. B.; Willis, A. C. *Acta Crystallogr., Sect. B* **1982**, *B38*, 443–448. (j) $[(C_{16}H_{28}N_4)Ni)_2(\mu\text{-}C_2O_4)]^{2+}[ClO_4]^-_2$ (1.503 (15) Å): Alcock, N. W.; Moore, P.; Omar, H. A. A. *Acta Crystallogr., Sect. C: Cryst. Struct. Commun.* **1987**, *C43*, 2074–2076.

(40) $Cp_2Ti(C_2O_4)$ (1.577 (7) Å): Doppert, K.; Sanchez-Delgado, R.; Klein, H. P.; Thewalt, U. *J. Organomet. Chem.* **1982**, *233*, 205–213.

(41) $Cs[Ti(C_2O_4)_2(H_2O)_3]\cdot 2H_2O$ (1.529 (6) Å): Drew, M. G. B.; Eve, D. J. *Acta Crystallogr., Sect. B* **1977**, *B33*, 2919–2921.

(42) (a) Alvalca, L.; Villa, A. C.; Manfredotti, A. G.; Mangia, A.; Tomlinson, A. A. G. *J. Chem. Soc., Dalton Trans.* **1972**, 391–395. (b) Sletten, J. *Acta Chem. Scand., Ser. A* **1983**, *A37*, 569–578. (c) Julve, M.; Faus, J.; Verdaguer, M.; Gleizes, A. *J. Am. Chem. Soc.* **1984**, *106*, 8306–8308. (d) Julve, M.; Verdaguer, M.; Gleizes, A.; Philoche-Levisalles, M.; Kahn, O. *Inorg. Chem.* **1984**, *23*, 3808–3818. (e) Kahn, O. *Angew. Chem., Int. Ed. Engl.* **1985**, *24*, 834–850, and references cited therein. (f) Real, J. A.; Borras, J.; Solans, X.; Font-Altaba, M. *Transition Met. Chem. (London)* **1987**, *12*, 254–256. (g) Bencini, A.; Fabretti, A. C.; Zanchini, C.; Zannini, P. *Inorg. Chem.* **1987**, *26*, 1445–1449.

(43) A theoretical examination (Jordan, K. D. *J. Chem. Phys.* **1984**, *88*, 2459–2465) of the $Li_2(C_2O_4)$ and $Na_2(C_2O_4)$ molecules calculated from 3-21G basis sets revealed that the D_{2h} complexes in which the individual alkali-metal atoms are chelated to two oxygen atoms from the two different CO_2 moieties are much more stable than those with the individual alkali-metal atoms chelated to two oxygen atoms from the same CO_2 group. The optimized geometry for the energetically preferred side-on bis(alkali metal–dioxo) chelated lithium and sodium oxalate molecules possessed C–C bond lengths of 1.576 and 1.594 Å, respectively. A structural refinement (Reed, D. A.; Olmstead, M. M. *Acta Crystallogr., Sect. B* **1981**, *B37*, 938–939) of crystalline $Na_2(C_2O_4)$ at 140 K with X-ray diffractometry data revealed the oxalate ion of crystallographic C_i-$\bar{1}$ site symmetry to be planar within experimental error with a C–C bond length of 1.568 (4) Å and two independent C–O bond lengths of 1.253 (3) and 1.265 (3) Å.

energy metal d orbitals and the majority of the occupied C_2O_4 orbitals. The overlap between these ligand orbitals and the metal d orbitals is small but does give rise to four σ-, one π-, and one δ-type interactions. The σ-type interactions are ligand $b_{1u}(a_u)$–dimetal d_{yz}, ligand $b_{2u}(b_u)$–dimetal d_{z^2}, ligand $b_{3g}(b_g)$–dimetal d_{yz}, and ligand $a_g(a_g)$–dimetal d_{z^2}. The π interaction is ligand $b_{1g}(a_g)$–dimetal d_{xz}, and the δ interaction is a ligand $a_u(a_u)$–dimetal d_{xy} overlap. The C_2X_4 ligand orbitals are designated by their representations under D_{2h} symmetry and, in parentheses, by their representations under assumed C_{2h}–$2/m$ symmetry (as a trans isomer) in order to facilitate a comparative analysis with **1**.

The oxalate-bridged molecule possesses two accidently degenerate HOMOs, each having greater than 90% metal character with the remaining percentage made up of Cp ring orbital character. The SHOMO (second highest occupied molecular orbital) is a metal–ligand bonding orbital composed of a σ interaction between the filled a_g C_2O_4 orbital and the (formally) vacant dimetal d_{z^2} orbitals. The LUMO in the C_2O_4-bridged complex is a metal–ligand π-bonding orbital made up of the ligand b_{3u} (b_u) (the LUMO of $C_2O_4^{2-}$) and dimetal d_{xz} orbitals.

Magnetic susceptibility and EPR studies of **2** showed that the molecule contains two unpaired electrons, one on each Ti center.[17] The molecular orbital calculations indicate that the unpaired electron on each d^1 Ti(III) occupies an orbital that is in the plane of the TiO_2 unit but has most of its electron density perpendicular to the line bisecting the two oxygens (see Figure 6a). This result agrees with previous results of Fenske–Hall MO calculations by Petersen et al.[34] on two Cp_2VX_2 molecules ($X_2 = S_5$, Cl_2) where the d^1 V(IV) atom was found to have its unpaired electron in a MO localized in the VS_2 (or VCl_2) plane perpendicular to the S---S (or Cl---Cl) bisector. Their orbital analysis is also in accordance with a subsequent theoretical analysis by Lauher and Hoffmann.[44]

The existence of an unpaired electron on each of the two symmetry-related Ti(III) atoms in **2** (cis isomer, $\alpha = 11.4°$) is a consequence of the pseudodegeneracy of the two half-filled HOMOs. The small energy separation (ca. 0.2 eV) between these two frontier MOs arises from the fact that they possess only 1% and 5% of C_2O_4-bridging ligand character. The two MOs can be viewed as symmetric (ϕ_s) and antisymmetric (ϕ_a) combinations of the symmetry-equivalent titanium-based orbitals. Hay, Thibeault, and Hoffmann[45] have shown, for d^9 Cu(II) binuclear complexes with oxalate-bridging ligands,[46] that antiferromagnetic coupling (stabilization of the singlet ground state) is a function of the square of the energy difference between the symmetric ϕ_s and the antisymmetric ϕ_a MO combinations. Hence, the results of our calculations on the oxalate-bridged dititanium molecule are in accordance with the weak antiferromagnetic interaction (which would imply a small energy difference between ϕ_s and ϕ_a) that has been experimentally measured by Hendrickson, Stucky, and co-workers.[17]

Molecular Orbital Analysis of $(Cp_2Ti)_2(\mu\text{-}C_2S_4)$. A molecular orbital diagram for $(Cp_2Ti)_2(\mu\text{-}C_2S_4)$, for which the observed α is 46.5°, is shown in Figure 5a. The five lower energy metal–ligand interactions between the filled low-lying C_2S_4 orbitals and corresponding dititanium d AOs are analogous in symmetry designation to those discussed previously for **2**. Because of the large out-of-plane trans folding of the two TiS_2 planes with respect to the $S_2C_2S_2$ plane, there is no combination of metal–ligand orbitals that has the proper symmetry to interact with the ligand orbitals in a pure σ, π, or δ fashion.

Figure 5a reveals two major ligand–metal bonding interactions in this complex. Based on the coordinate system shown in Figure 1c and the ligand orbitals shown in Figure 3, these two interactions can be identified as the following: a donation from the ligand b_{3g} σ orbital (the HOMO of $C_2S_4^{2-}$) to a (formally) empty dititanium d_{yz} orbital and a back-donation from the two half-occupied dititanium $d_{x^2-y^2}/d_{z^2}$ hybrid orbitals to the empty b_{3u} π-ligand orbital (the LUMO in $C_2S_4^{2-}$). This latter metal–ligand bonding interaction constitutes the HOMO of **1**. Its π-ligand orbital component (the LUMO of $C_2S_4^{2-}$) is S–C antibonding and C–C bonding (Figure 6b). Hence, occupation of this HOMO corresponds to the two electrons donated from the metal atoms being delocalized over the C_2S_4 ligand: this ligand delocalization significantly strengthens the C–C bond and shortens its bond distance. The LUMO of **1** is almost completely localized on the metal and has less than 10% ligand character. The HOMO–LUMO energy gap of >2 eV results in this molecular complex being diamagnetic, as observed.

The most important feature of the electronic structure of **1** is the availability of the empty C_2S_4 b_{3u} orbital to participate in bonding of the complex. The favorable energy match between this ligand orbital and the two half-occupied metal hybrid orbitals allows a strong bonding interaction to occur. If the metal atoms were in the plane of the C_2S_4 ligand, the metal donor and ligand acceptor orbitals would be orthogonal to one another; however, the experimentally observed folding by 46.5° of the Cp_2Ti fragments out of the C_2S_4 plane allows the metal hybrid orbitals to overlap with the ligand b_{3u} orbital. The considerable interaction of the metal and bridging-ligand orbitals that results from the large trans folding leads to the electron-pair delocalization of the previously unpaired metal electrons throughout the $TiS_2C_2S_2Ti$ core.

Comparative Natural Population Analysis of the Electronic Structures of $(Cp_2Ti)_2(\mu\text{-}C_2O_4)$ (2) and $(Cp_2Ti)_2(\mu\text{-}C_2S_4)$ (1) and Resulting Implications. A comparison of the charges of the Ti, Cp, and C_2X_4 fragments in **1** and **2** obtained from a natural population analysis versus those obtained from a Mulliken population analysis is of particular interest in delineating their electronic structures. On the basis of calculated Mulliken atomic populations, the charges for each Ti atom are +0.65 in **1** and +0.79 in **2**, while the total charges for each of the four Cp ligands are −0.19 in **1** and −0.27 in **2**. These values give rise to nearly equivalent total charges of −0.54 for the C_2S_4 ligand in **1** and −0.50 for the C_2O_4 ligand in **2**. On the other hand, the natural bond orbital method, which provides a more realistic assessment of atomic charges, gives considerably higher, similar positive charges for each titanium atom of +1.29 in **1** and +1.33 in **2**. However, the smaller total charge for each of the Cp ligands of −0.365 in **1** compared to that of −0.43 in **2** results in a total charge of −1.12 for the C_2S_4 ligand in **1** compared to that of −0.94 for the C_2O_4 ligand in **2**. This delocalization of a significantly greater negative charge onto the C_2S_4 ligand in **1** is completely consistent with the proposed description (based upon experimental data) that the C_2S_4 ligand conforms to a nonintegral oxidation state between a $C_2S_4^{2-}$ dianion interacting with two d^1 Ti(III) Cp_2Ti^+ moieties and an ethylenetetrathiolate $C_2S_4^{4-}$ tetraanion interacting with two d^0 Ti(IV) Cp_2Ti^{2+} moieties. In other words, **1** possesses an electron-delocalized configuration such that an integral oxidation state cannot be assigned (under a valence-bond formalism) to the bridging C_2S_4 ligand and two Ti atoms. In contrast, the oxalato-bridged **2** possesses an electron-localized configuration involving the interaction of a $C_2O_4^{2-}$ dianion with two d^1 Ti(III) Cp_2Ti^+ fragments. Both the geometry and experimentally determined spin-only paramagnetism of **2** reinforce this unambiguous assignment of a d^1 Ti(III) oxidation state to each metal.

Although an ionic salt of the ethylenetetrathiolate $C_2S_4^{4-}$ tetraanion has not been isolated, such a species would be expected to possess a distinct C–C double bond. The electron-rich olefin, $C_2(SMe)_4$, was shown by Lappert and co-workers[47] to form a

---

[44] Lauher, J. W.; Hoffmann, R. *J. Am. Chem. Soc.* **1976**, *98*, 1729–1742.

[45] Hay, P. J.; Thibeault, J. C.; Hoffmann, R. *J. Am. Chem. Soc.* **1975**, *97*, 4884–4899.

[46] A considerable number of (μ-oxalato)copper(II) binuclear complexes have been extensively investigated[42] in order to determine the nature of the magnetic interactions between the two d^9 Cu(II) that are chelated in a side-on fashion to the bridging oxalate ligand. In all of these complexes the central $CuO_2C_2O_2Cu$ core is essentially planar.

[47] (a) Centinkaya, B.; Hitchcock, P. B.; Lappert, M. F.; Pye, P. L. *J. Chem. Soc., Chem. Commun.* **1975**, 683–684. (b) Cetinkaya, B.; Hitchcock, P. B.; Lappert, M. F.; Pye, P. L.; Shaw, D. B. *J. Chem. Soc., Dalton Trans.* **1979**, 434–440. (c) Lappert, M. F.; Shaw, D. B.; McLaughlin, G. M. *J. Chem. Soc., Dalton Trans.* **1979**, 427–433.

side-on metallo–dithio adduct, *cis*-$Cr(CO)_4[C_2(SMe)_4]$, with a C–C bond length of 1.335 (9) Å and (with S–Me bond cleavage) a side-on bis(metallo–dithio) complex, $[(Et_3P)ClPt]_2(\mu\text{-}C_2(S)_2(SMe)_2)$, with a C–C bond length of 1.34 (4) Å. The bridging C_2S_4 ligand in $Fe_4(CO)_{12}(C_2S_4)$, in which two centrosymmetrically related $Fe_2(CO)_6$ moieties are each attached to the bridging C_2S_4 ligand by both iron atoms in an end-on bis(bimetallo–dithio) fashion, was formally regarded as a derivative of ethenetetrathiol rather than a tetrathiooxalate ligand on the basis of its C–C and C–S bond lengths of 1.33 (1) and 1.77 Å (av), respectively.[2] The molecular parameters of $(Cp^*Ni)_2(\mu\text{-}C_2S_4)$ (C–C, 1.360 (11) Å; C–S, 1.718 (3) Å),[3] $(Cp^*Co)_2(\mu\text{-}C_2S_4)$ (C–C, 1.369 (11) Å; C–S, 1.725 Å (av)),[4] and *trans*-$(Cp^*(OC)Fe)_2(\mu\text{-}C_2S_4)$ (C–C, 1.430 (9) Å; C–S, 1.701 Å (av))[4] suggest that the bridging C_2S_4 ligand in the nickel and cobalt complexes can also be considered as an ethylenetetrathiolate tetraanion linked to two d^7 Ni(III) $CpNi^{2+}$ and two d^6 Co(III) $CpCo^{2+}$ moieties, respectively. Nevertheless, MO calculations[4] performed with the Fenske–Hall model[18] on these three complexes revealed a considerable variation in electron delocalization consistent with the premise that the C_2S_4 ligands in the cobalt and nickel complex are near (but not at) the limiting case corresponding to an ethylenetetrathiolate tetraanion.

A comprehensive structural–magnetic investigation and molecular orbital analysis of the first known (μ-tetrathiooxalato)copper(II) binuclear complex, $[AsPh_4]^+{}_2[((C_3OS_4)Cu)_2(\mu\text{-}C_2S_4)]^{2-}$, were recently reported by Vicente et al.[48] The two centrosymmetrically related copper atoms were found to possess a distorted square-planar coordination (torsional angle 28.3°). This deviation from planarity of the four-coordinate copper atoms was attributed to a second-order Jahn–Teller effect and was correlated with the C–C bond strength of the C_2S_4 ligand in the essentially planar $CuS_2C_2S_2Cu$ core. The observed C–C distance of 1.47 (1) Å for the C_2S_4-bridged ligand is equal to that of 1.46 (2) Å determined[38] for the highly nonplanar $C_2S_4{}^{2-}$ anion (torsional angle 79.5°) in the hydrated tetraphenylphosphonium salt but smaller than that of 1.531 (8) Å found[49] for the planar, side-on bridging C_2S_4 ligand (viewed as a dianion) in a centrosymmetric d^{10} Cu(I) complex, $[(Ph_3P)_2Cu]_2(\mu\text{-}C_2S_4)$. On the basis of these bond-length variations, Vicente et al.[48] concluded that the C_2S_4-bridged ligand in the $[((C_3OS_4)Cu)_2(\mu\text{-}C_2S_4)]^{2-}$ dianion can also be formally considered as $C_2S_4{}^{2-}$ and not as a $C_2S_4{}^{4-}$ anion. This formulation of an integral 2– oxidation state for the C_2S_4 ligand results in a d^9 Cu(II) oxidation state for each copper atom. The mean C–S bond length of 1.675 Å in this binuclear Cu(II) complex is virtually identical to that in the above-mentioned (μ-tetrathiooxalato)copper(I) binuclear complex and slightly smaller than that of 1.702 Å in the "free" $C_2S_4{}^{2-}$ anion. Magnetic measurements led to a lower limit estimate for the antiferromagnetic coupling constant of $|J| > 800\ cm^{-1}$, which is the largest one in a series of similar bis(bidentate) bridges (viz., oxalato, oxamido, dithiooxamido, and tetrathiooxalato). This large antiferromagnetic coupling constant was rationalized on the basis of extended Hückel-type MO calculations.[48]

The combined experimental–theoretical results emphasize that the tetrathiooxalate ligand in **1** is a better acceptor of electron density than the oxalate ligand in **2** such that in **1** this ligand can be regarded as tetrathiolene-like. The mean C–C distance of 1.41 Å supports these conclusions in being intermediate between a normal double- and single-bond distance.

The titanium orbital contributions to the HOMOs in both **1** and **2** involve the same type of valence $d_{z^2}/d_{x^2-y^2}$ AOs. The major difference between the electronic structures of **1** and **2** lies in the ability of the b_{3u} π-acceptor orbital of C_2S_4 to interact with the antisymmetrical dititanium combination of these Ti $3d_{z^2}/d_{x^2-y^2}$ AOs. This empty b_{3u} C_2X_4 π orbital (the LUMO in a "free" $C_2X_4{}^{2-}$) is considerably lower in energy for X = S and is thereby available to accept electrons from the titanium atoms. Since the resulting titanium–C_2S_4 orbital overlap in this HOMO would be zero in a planar $TiS_2C_2S_2Ti$ system, the observed large trans folding in **1** is necessary in order for the partially occupied metal orbitals to overlap extensively with the π system of the C_2S_4 unit. This interaction accounts for the pairing up of the previously unpaired electrons on the metals in harmony with the observed diamagnetism of the molecule.

The corresponding b_{3u} π-acceptor orbital of the oxalate ligand is too high in energy to interact with the metal d orbitals. For this reason, **2** adopts an electronic structure that is nearly that of a planar $TiO_2C_2O_2Ti$ system. The unpaired electron on each Ti(III) remains unpaired, and the symmetrical and antisymmetrical sets of Ti $3d_{z^2}/d_{x^2-y^2}$ AOs that these electrons occupy make up the essentially degenerate HOMOs of the molecule.

Results Based on Alternative Geometries. The experimentally determined geometry of **1** indicates a trans folding of the Cp_2Ti fragments out of the C_2S_4 plane by 46.5°. The folding angle (α) for **2**, however, is observed to be 11.4°. In order to determine to what extent a change in geometry of a given molecule affects its electronic structure, calculations were performed on **1** and **2** with a variety of different values for α. For each calculation, the Ti–X and Ti–Cp distances were held constant as the two Cp_2Ti fragments were rotated about the X- -X vectors. We have investigated the electronic structures of the molecules in their experimentally determined geometries (**1**, α = 46.5°; **2**, α = 11.4°). Additionally, we have examined **2** with a trans-folding angle of 46.5°, **1** with a trans-folding angle of 11.4°, and both molecules with α = 0.0° (i.e., a totally planar $MX_2C_2X_2M$ unit).

The results of the calculations for $(Cp_2Ti)_2(\mu\text{-}C_2S_4)$ with α = 11.4° are shown in Table III and Figure 5. The main feature observed here is a lowering of the orbital energies of the bridging ligand relative to those of the metals. This leads to more charge transfer from the metal atoms to the C_2S_4 ligand. There is also more symmetry-allowed mixing of the ligand orbitals than was observed at α = 46.5°. The HOMO is comprised of metal $d_{x^2-y^2}$ and ligand b_{3u} orbital character as before; however, the energy is ~1 eV higher, indicative of the smaller overlap between these two orbitals.

The results of the calculations for $(Cp_2Ti)_2(\mu\text{-}C_2O_4)$ at α = 46.5° are shown in Figure 4b. The prominent feature here is an increase in energies for the ligand bonding orbitals relative to those for metal d orbitals. Less obvious from the energy diagram but apparent upon examination of the overlap populations is the lessening of the overlap between the Ti atoms and the C_2O_4 ligand. The total metal–ligand overlap population (TOP) is substantially decreased upon going from α = 11.4° (metal–ligand TOP = 1.35) to α = 46.5° (metal–ligand TOP = 1.08). This is due mainly to the decreased interactions of the d_{yz} metal orbitals with the in-plane π C_2O_4 orbitals and the d_{xz} and d_{xy} metal orbitals with the out-of-plane π C_2O_4 orbitals.

When the folding angle is decreased from 11.4° to 0.0° for $(Cp_2Ti)_2(\mu\text{-}C_2O_4)$, no substantial change in the electronic structure of the molecule occurs. The orbital energies, percent compositions, and overlap populations are nearly unchanged. One is left to conclude from this that the 11° folding angle represents a relatively small deviation from planarity that leads to a minor perturbation in the electronic structure.

The electronic structure of **1** shows a substantial change upon going from α = 46.5° or 11.4° to α = 0.0°. The C_2S_4 ligand b_{3u} orbital continues to play a very important role in the bonding of the molecule. The ideal energy match of this ligand orbital with the Ti d orbitals, which apparently is the driving force in the trans folding of **1** and its resulting dimagnetism, is still observed in the planar system. However, in the planar system the metal orbitals that contain the unpaired electron are orthogonal to the ligand acceptor orbital, b_{3u}. The metal orbitals that are of the proper symmetry to interact with this ligand orbital are the vacant d_{xz} orbitals. This leads to two very different possibilities for the electronic structure of the molecule in a planar configuration.

In the situation where the ligand b_{3u} fragment orbital is slightly lower in energy than the set of $d_{x^2-y^2}/d_{z^2}$ hybrid metal orbitals, two electrons must be formally transferred to the ligand b_{3u} orbital.

---

(48) Vicente, R.; Ribas, J.; Alvarez, S.; Segui, A.; Solans, X.; Verdaguer, M. *Inorg. Chem.* **1987**, *26*, 4004–4009.

(49) Hansen, L. K.; Sieler, J.; Strauch, P.; Dietzsch, W.; Hoyer, E. *Acta Chem. Scand., Ser. A* **1985**, *A39*, 571–575.

The (now) occupied b_{3u} orbital can interact with the vacant d_{xz} metal orbitals forming the HOMO. The metal d_{xz} orbital lies at higher energy, however, due to an antibonding interaction with the Cp rings; hence, the bonding interaction with the ligand b_{3u} orbital will be weak and the HOMO will be mainly ligand in character. The LUMOs in this case are the set of pseudodegenerate $d_{x^2-y^2}/d_{z^2}$ hybrid metal orbitals that formerly held the unpaired electrons on the Ti centers. This situation leads to a diamagnetic molecule but requires a complete two-electron transfer from the two metal atoms to the ligand, making the molecule a $C_2S_4^{4-}$ tetraanion interacting with two d^0 Ti(IV) Cp_2Ti^{2+} fragments.

An alternative electronic structure will occur if the metal d orbitals are slightly lower in energy than the C_2S_4 ligand b_{3u} orbital. In this case the HOMOs of the molecule are the set of pseudodegenerate $d_{x^2-y^2}/d_{z^2}$ orbitals, each singly occupied, while the LUMO is the bonding combination of ligand b_{3u}–dimetal d_{xz}. This leads to a paramagnetic molecule as observed for **2**, the main difference being that the HOMO–LUMO gap is much less in the C_2S_4-bridged **1** than in the C_2O_4-bridged **2**.

Theoretical Rationale for the Observed Electrochemistry. Experimental investigations have established that the C_2X_4-bridged dititanium compounds exhibit contrasting electrochemical behavior. Floriani and co-workers[15] reported that the $C_2(NR)_4$-bridged dititanium complex undergoes a two-electron oxidation that, they concluded, affects only the oxidation state of each of the metal centers. Cyclic voltammetric studies in our laboratory revealed that **2** also displays reversible oxidative behavior. In contrast, **1** exhibits no reversible oxidations although it does undergo two quasi-reversible one-electron reductions. The characteristic redox behavior of these compounds can be rationalized by our molecular orbital calculations and, in fact, provides experimental verification of our preceding discussions.

A qualitative explanation for the observed electrochemistry can be obtained from an analysis of the frontier orbitals if one assumes the ordering (as well as character) of the molecular orbitals remains essentially unaltered upon oxidation or reduction. The effect of oxidation or reduction can also be examined by analyzing the total overlap populations between atoms subsequent to a molecular orbital computation on the appropriate charged species. These calculations enable one to predict (qualitatively) the changes in bond length that may occur upon oxidation or reduction. Such a TOP analysis requires that the geometries for the cations and anions as well as the basis set used remain identical with those used for the neutral parent and that only the charges are altered. In this way, an increase in the TOP between two atoms is indicative of greater electron density between the two atoms, and consequently a decrease in the bond length would be predicted. The total valence overlap populations for $[(Cp_2Ti)_2(\mu\text{-}C_2O_4)]^{2+}$, $[(Cp_2Ti)_2(\mu\text{-}C_2S_4)]^{2+}$, and their neutral parents are presented in Table IV.

Table IV. Prediction of Bond Length Changes in the Neutral $[(Cp_2Ti)_2(\mu\text{-}C_2X_4)]^n$ Series (X = S, O; n = 0) upon Oxidation (n = +2) Based on Changes of Total Overlap Populations[a,b]

	TOP		predicted bond length change
	n = 0	n = +2	
	X = S		
S–Ti (9 valence AOs)[b]	1.18	1.10	increase
S–Ti (5 3d AOs)	0.55	0.48	increase
S–C	1.63	1.83	decrease
C–C	1.21	1.07	increase
	X = O		
O–Ti (9 valence AOs)[b]	0.79	0.88	decrease
O–Ti (5 3d AOs)	0.33	0.40	decrease
O–C	1.97	1.99	no change
C–C	0.87	0.85	no change

[a] $\text{TOP}(k,l) = \sum_i\sum_{r_k}\sum_{s_l}2N(i)C_{r_k}C_{s_l}S(r_k,s_l)$, where C_{r_k} and C_{s_l} are coefficients of valence orbitals on atoms k and l in the *i*th MO, populated with $N(i)$ electrons. $S(r_s,s_l)$ denotes orbital overlap; the first summation is over all occupied MOs. It is noteworthy that TOP is a measure of the degree of covalency (i.e., bonding electron density) between atoms. [b] For comparative analysis, TOP values for each Ti–X atomic pair are given both for the five 3d, one 4s, and three 4p valence AOs on Ti and for only the five 3d AOs.

The electronic structure of the oxalate species, **2**, strongly suggests the possibility of reversible oxidation. As shown in Table III, the HOMOs of **2** are two accidentally degenerate molecular orbitals each containing one electron. These orbitals, which are primarily (89%) metal in character, are energetically removed from the ligand orbitals and are only slightly stabilized (<0.2 eV) relative to the Ti 3d orbital level. The small stabilization energy associated with the HOMOs, as well as the absence of bridging ligand character in these molecular orbitals, implies that these electrons are not essential to the bonding of the complex and might be easily removed. Furthermore, removal of electrons from principally metal-based molecular orbitals serves to lessen the electron density on the metals and lower the dititanium 3d energy levels relative to the filled low-lying C_2O_4 orbitals, thereby strengthening the metal–ligand bonding by providing better metal orbital–ligand orbital energy matching. These bonding considerations account for the TOP analysis (Table IV) indicating that the mean Ti–O bond length would be shorter in the dication of **2** relative to that in the neutral parent but that the C–O and C–C bond lengths of the bridging ligand would be relatively unaffected. Although no structural data are available (as yet) for the dication, this bond length prediction is completely compatible with the Ti–O distances in the d^0 Ti(IV) $Cp_2Ti(C_2O_4)$[40] being 0.16 Å smaller than those in **2**.[50,51]

The electronic structure of the C_2S_4-bridged **1** reinforces the electrochemical data as strongly mitigating against **1** undergoing reversible oxidation to any cationic species. In contrast to the HOMOs of **2**, the HOMO of **1** contains a substantial amount (~60%) of bridging ligand character and is strongly metal–ligand bonding. The molecular orbital analysis of the neutral dimer given previously shows that the HOMO is of prime importance in the dititanium–C_2S_4 interactions. Removal of one or two electrons from this orbital via oxidation should severely weaken this dimetal–C_2S_4 interaction. The results of MO calculations for the nonexistent cations of **1** expectedly show a decrease in the TOP between titanium and sulfur atoms and between the two carbon atoms in the bridging ligand but an increase in the TOP between the sulfur and carbon atoms. This leads to a prediction of increased Ti–S bond lengths, an increased C–C bond length, and decreased S–C bond lengths in the hypothetical cations relative to those in the neutral parent.

The key point in this discussion is that the fundamental electronic differences between the tetrathiolate-bridged and oxalate-bridged species discussed in this work are the origin of the contrasting oxidative behavior of these two molecules. By virtue of a low-lying acceptor orbital on the C_2S_4 ligand, the HOMO of **1** is primarily metal–ligand bonding. Thus, its electrons cannot be removed without major electronic rearrangement. In contrast, the C_2O_4 ligand in **2** does not possess any orbitals in the vicinity

---

(50) The prediction of smaller Ti–O bond lengths upon oxidation of **2** to its dication due to the formal conversion of the two d^1 Ti(III) into two d^0 Ti(IV) by removal of two electrons from the half-filled HOMOs is in agreement with structural data[40] for the d^0 Ti(IV) $Cp_2Ti(C_2O_4)$. The Ti–O distances of 1.995 (4) and 2.003 (3) Å in this dicyclopentadienyl(oxalato)titanium(IV) molecule are 0.16 Å smaller than those in **2**. The side-on Ti–dioxo chelation of the planar $C_2O_4^{2-}$ ligand with the Cp_2Ti^{2+} fragment products a small folding angle of α = 2.8° due to the Ti(IV) being displaced by only 0.08 Å from the mean plane of the oxalate atoms. Further experimental evidence that the unpaired electron in each d^1 Ti(III) of **2** causes a lengthening (and hence weakening) of the Ti–O bonds via a "charge effect"[51] is provided from a structural determination[41] of the $[Ti(C_2O_4)_2(H_2O)_3]^-$ monoanion as the hydrated Cs^+ salt. The d^1 Ti(III) in this anion of crystallographic C_s-*m* site symmetry has a seven-coordinate pentagonal-bipyramidal oxygen environment with two water oxygen atoms at axial positions and the third water oxygen atom and four oxygen atoms from the two bidentate oxalate ligands at equatorial positions. The two independent Ti–O(oxalate) bond lengths of 2.115 (3) and 2.134 (3) Å in this monoanion are expectedly similar to those in **2**.

(51) (a) Maj, J. J.; Rae, A. D.; Dahl, L. F. *J. Am. Chem. Soc.* **1982**, *104*, 3054–3063. (b) Cirjak, L. M.; Ginsburg, R. E.; Dahl, L. F. *Inorg. Chem.* **1982**, *21*, 940–957. (c) Kubat-Martin, K. A.; Barr, M. E.; Spencer, B.; Dahl, L. F. *Organometallics* **1987**, *6*, 2570–2579.

of the metal d orbitals. Thus, the accidentally degenerate HOMOs in this species contain two unpaired electrons that can be removed without rupturing the complex.

Cyclic voltammetric and EPR studies of **1** clearly indicate the presence of two one-electron reduction processes that strictly are quasi-reversible. Quasi-reversibility most often is an indication of slow electron transfer, which can be caused by geometrical or conformational changes in the molecule before, during, or after electron transfer.[52] Fenske–Hall calculations were performed on the anions of **1**. The reduction of **1** to its monoanion results in an electron being added to the LUMO, which is primarily metal-based (84%) with some Cp (14%) and C_2S_4 (2%) character. This metal-based orbital is not strongly antibonding and could accommodate an extra electron.

Calculations on the dianion indicate that a geometrical arrangement may be occurring in the molecule. We are continuing to investigate the intriguing reduction chemistry of the C_2S_4-bridged titanium dimer with hope of isolating these anions for structural investigation.

Acknowledgment. This research was generously supported by the National Science Foundation. We are particularly pleased to acknowledge Professor Dick Fenske for several helpful discussions and Dr. Gary Wesenberg for his assistance with the VAX 8650 computer system. H.A.H. is especially grateful to Dr. Kimberly A. Schugart for her assistance in the initial use of the Fenske–Hall MO program. D.R.K. thanks Professor Frank Weinhold for fruitful discussions related to the natural bond orbital (NBO) procedure developed by him and his co-workers.

Registry No. 1, 109242-42-4; 2, 78452-81-0; $C_2O_4^{2-}$, 338-70-5; $C_2S_4^{2-}$, 78906-82-8; $[(Cp_2Ti)_2(\mu\text{-}C_2Su)]^{2+}$, 136236-70-9; $[(Cp_2Ti)_2(\mu\text{-}C_2O_4)]^{2+}$, 136236-69-6.

---

[52] For an extensive discussion of conformation changes, isomerism, and electron transfer see: Evans, D. H.; McConnell, K. M. *Electroanal. Chem.* **1986**, *14*, 113–207.

Elemental Structures of the Heavy Main Group Atoms and the Second Moment Scaling Hypothesis

Stephen Lee

Contribution from the Department of Chemistry, The University of Michigan, Ann Arbor, Michigan 48109-1055. Received July 23, 1990

Abstract: We show that Hückel calculations, used in conjunction with second moment scaling, correctly predict the structure types in a given row of the main group atoms. We accurately predict the structure types of Cu, Zn, Ga, Ge, As, Se, Ag, Cd, In, Sn, Sb, Te, Tl, Pb, Bi, and Po. Only one significant error is observed in this series.

Introduction

The structure of the elements is a fundamentally important issue in solid-state chemistry and physics.[1] For this reason theoretical methods have been developed which quite accurately account for these structures. One particular theoretical triumph has been the use of pseudopotential methods.[2] Pseudopotential calculations are able to accurately predict the elemental phase transitions caused by increasing pressure. It has been found that pressure often induces elements to adopt the structure type of a heavier element which belongs to the same column of the periodic table. For example Si under pressure first adopts the white-Sn (w-Sn) structure and later under very high pressure adopts the fcc structure of Pb.[3] Therefore, pseudopotential calculations have generally been used in comparing elemental structure types which are found in a given column in the periodic table.

Much less work has been carried out in comparing the structure types found in a given row of the periodic table. One more recent exception to this is to be found in the work of Pettifor.[4] Pettifor has shown the tightbinding (or Hückel) method can resolve the structural preferences of the transition-metal series (from group 3 to group 10). One especial advantage of these Hückel calculations is that due to their calculational simplicity it is possible to determine the geometric origins of Hückel energetic effects.[5] However, the Hückel method has not been very widely applied to main group elemental structures. The principal difficulty is associated with coordination number (i.e., the number of near neighbors an atom possesses). The three main transition metal structure types (fcc, hcp, and bcc) all have uniformly high coordination numbers. This changes upon leaving the transition-metal block. For instance, while Cu and Zn are 12 coordinate, their neighbors Ga, Ge, and As are respectively 7, 4, and 3 coordinate. The problem is that in Hückel theory, coordination number is approximately proportional to Hückel band width, and band width directly affects Hückel energies. The results of a direct comparison of the Hückel energies of the Cu, Zn, Ga, Ge, and As structures would therefore be senseless.

Scaling Hypothesis

These difficulties in Hückel theory can be directly traced to the absence of repulsive terms in the Hückel Hamiltonian. As there are no repulsive energy terms, there are no forces in Hückel theory which keep the atoms away from one another. Unfortunately accurate calculation of repulsive interactions between the electrons in a system requires the use of multideterminental wave functions.[6] It is therefore difficult to devise a method which accurately calculates the effects of these inter-

---

[1] See: Donohue, J. *The Structure of the Elements*; Wiley: New York, 1974.

[2] (a) Heine, V.; Weaire, D. *Solid State Phys.* **1970**, *24*, 247. (b) Yin, M. T.; Cohen, M. L. *Phys. Rev. Lett.* **1980**, *45*, 1004. (c) Yin, M. T.; Cohen, M. L. *Phys. Rev. B* **1981**, *24*, 6121; **1982**, *26*, 5668.

[3] (a) Olijnyk, H.; Sikka, S. K.; Holzapfel, W. B. *Phys. Lett.* **1984**, *103A*, 137. (b) Hu, J. Z.; Spain, I. L. *Solid State Commun.* **1984**, *51*, 263. (c) Duclos, S. J.; Vohra, Y. K.; Ruoff, A. L. *Phys. Rev. Lett.* **1987**, *58*, 775. (d) Vohra, Y. K.; Brister, K. E.; Desgreniers, S.; Ruoff, A. L.; Chang, K. J.; Cohen, M. L. *Phys. Rev. Lett.* **1986**, *56*, 1944; Fahy, S. G.; Louie, S. G. *Phys. Rev. B* **1987**, *36*, 3373.

[4] (a) Pettifor, D. G. *Calaphad Comput. Coupling Phase Diagrams Thermochem.* **1977**, *1*, 305. (b) Pettifor, D. G. *J. Phys. C* **1970**, *2*, 366. (c) Duthie, J.; Pettifor, D. G. *Phys. Rev. Lett.* **1977**, *38*, 564. (d) Burdett, J. K. *J. Phys. Chem.* **1983**, *87*, 4368.

[5] (a) Ducastelle, F.; Cyrot-Lackman, F. *J. Phys. Chem. Solids* **1970**, *31*, 1295; **1971**, *32*, 285. (b) Gaspard, J. P.; Cyrot-Lackmann, F. *J. Phys. C* **1973**, *6*, 3077. (c) Burdett, J. K.; Lee, S. *J. Am. Chem. Soc.* **1985**, *107*, 3050, 3063.

[6] For a discussion of these techniques see: Szabo, A.; Ostlund, N. S. *Modern Quantum Chemistry*; Macmillan: New York, 1982.

0002-7863/91/1513-8611$02.50/0 © 1991 American Chemical Society